ESTIMATION OF TURBINE NOISE BENEFITS DUE TO ACOUSTICALLY TREATED OUTLET GUIDE VANES

Adolfo Serrano - Guillermo Torres

adolfo.serrano@itp.es, guillermo.torres@itp.es
ITP, Industria de Turbo Propulsores S.A., Madrid, Spain

ABSTRACT

This paper aims to assess via CFD the feasibility of using acoustic treatments over the Outlet Guide Vanes (OGVs) surfaces in a turbine. The CFD solver to be used is Mu^2s^2T that is an in-house suite of codes. In absence of a dedicated experiment, the capability of Mu^2s^2T for assessing this novel technology is investigated in two parts. First, CFD predictions of turbine tones are compared with measurements for a state of the art turbine including OGV. Second, the CFD liner prediction capability is assessed in two test cases: straight duct with uniform flow and fan noise test with a lined OGV.

Once the CFD capability is assessed and uncertainties understood, the treated OGV technology is investigated for a state of the art Low Pressure Turbine (LPT). The optimum liner characteristics are chosen by the construction of the usual cell depth vs porosity charts for a straight duct. Selected candidate is simulated over the suction or pressure OGV sides and the differences are discussed. Overall tone noise reduction deltas are provided and compared with existing technology consisting in having acoustic treatments over the hot nozzles downstream the OGV.

NOMENCLATURE

OPENAIR	OPtimisation for low Environmental Noise impact
SILENCE(R)	Signifantly Lower Community Exposure to Aircraft Noise
ANTLE	Affordable Near Term Low Emissions
TSTF	Twin Shaft Test Facility
UFFA	Universal Facility for Acoustics
CFD	Computational Fluid Dynamics
OGV	Outlet Guide Vane
RANS	Reynolds Averaged Navier-Stokes
URANS	Unsteady Reynolds Averaged Navier-Stokes
LRANS	Linearized Reynolds Averaged Navier-Stokes
LPT	Low Pressure Turbine
i	Imaginary Part
y^+	Dimensionless wall distance
B	Number of Blades
V	Number of Vanes
k	Any integer in the Tyler & Sofrin rule
BPF	Blade Passing Frequency
PWL	Acoustic Power
dB	deciBel
PNLT	Perceived Noise Level with Tone correction

INTRODUCTION

Low Pressure Turbine (LPT) noise can be an important contributor to the overall perceived aircraft level (Nesbitt, 2011). Continuous efforts for having quieter but also light and efficient turbines make necessary the development of advanced technologies in order to have more competitive products as a whole. Within this context, the use of acoustic treatments over turbine OGVs can be an opportunity. Broszat (2011) gets promising results when assessing OGVs with liners over the inner and outer casings. Acoustic treatment over the OGV airfoil may be an additional opportunity, as recently demonstrated for fan noise (Reba et al. 2008, Elliot et al. 2009, Jones et al. 2009). However, there has not been found previous studies addressing its feasibility in turbines, and fan noise results might not be directly applicable due to several reasons. First, the OGV role in turbine noise generation is very different from that in fans (Serrano, 2008), and the liner acoustic performance might be different as well. Other important matters are mechanical constrains, size limitations and aerodynamic implications. Since this is a first approach for assessing the acoustic feasibility, these other issues are not covered here

This work starts with a short description of the CFD tool used in the assessment together with the numerical models to be used for tone noise estimation. In absence of a dedicated experiment, a reliable prediction of treated turbine OGVs requires assessing the CFD capability for predicting turbine tones and liner attenuation. The first is assessed by comparing CFD against measurements from a 4-stage full scale turbine rig including the OGV. The second is assessed in two test cases, a simple straight duct, where CFD results are tested with a semi-analytical tool, and a fan test including a lined OGV test where predictions are compared against measurements. The last section estimates the attenuation for a state of the art LPT. Noise sources are estimated for one unique working condition located in between Landing and Take-Off aimed to have estimations representative of these conditions. The sources emerging from the Turbine, estimated via CFD, are the input for constructing the usual cell depth vs porosity charts as if it were a straight duct, and the optimum liner characteristics are derived. The convenience of using acoustic treatment whether in the suction or pressure side is investigated and overall tone noise reduction estimated.

CFD AND MODELS DESCRIPTION: The Mu^2s^2T Suite

Mu^2s^2T is an in-house suite of solvers with hybrid unstructured grids to discretize the spatial domain and an edge-based data structure to compute the fluxes. A second-order numerical scheme forms the spatial discretization scheme. The time-marching technique has been implemented with an explicit five-stage Runge-Kutta. Multigrid techniques are used to accelerate steady state convergence.

Turbomachinery noise can be predicted with Mu^2s^2T using two different models: Linearized Reynolds Averaged Navier-Stokes (LRANS), and Unsteady Reynolds Averaged Navier-Stokes (URANS). The LRANS method is linear; it assumes the unsteady field is small compared to the time averaged or main one. Therefore, noise is estimated in two steps: the first is set of RANS computations for each row assuming that the flow is steady. Then, the wakes and potential field for each upstream row are linearized and transmitted through the downstream row using Mu^2s^2TL, which is a frequency domain CFD solver that resolves the linearized RANS equations over the previously calculated main flow. URANS model resolves the unsteady equations in time domain using the dual time step technique (Burgos et al, 2011). Computational cost is considerably increased but retains non-linear multi-stage effects. Fernandez et al. (2011, 2012) describes in detail the LRANS and URANS models used here and, when investigating a set of

2D, 3D, compressor and turbine representative models, concludes that the two models conduces to similar results provided the distance between rows is sufficiently high.

The capability of both Mu^2s^2T and Mu^2s^2TL to perform unsteady simulations in turbomachines has been already demonstrated (Escribano et al., 2003, Corral et al., 2003, Burgos et al., 2011 and Fernández et al., 2012).

TURBINE TONE PREDICTION CAPABILITY

A proper estimation of turbine OGV liner benefits requires the assessment on the CFD capability for predicting turbine tones. This is done by comparing noise measurements from a turbine rig with CFD estimations. The test occurs at the Twin Shaft Test Facility (TSTF) located in Rolls-Royce (UK) in 2005, and funded by the SILENCE(R) European Programme. The TSTF is a 'cold' facility, with inlet working temperatures from 430K to 460K and able to test full-scale large civil turbofan LPT rigs. Noise measurements are taken downstream the rig, with 27 pressure sensors located in a cylindrical device able to rotate. Details on the facility and how the measurements are taken and processed can be followed in Serrano et al. (2007, 2011). The vehicle is the ANTLE LPT Cold Flow Rig, which is a 4-stage, full scale, state of the art LPT. ANTLE LPT is a high loaded turbine (Vazquez et al., 2003) which targets the same efficiency of the Rolls-Royce Trent 500 LPT, but with one less stage and 25% reduction over cost and weight. Figure 1(left) shows the lay out of the turbine.

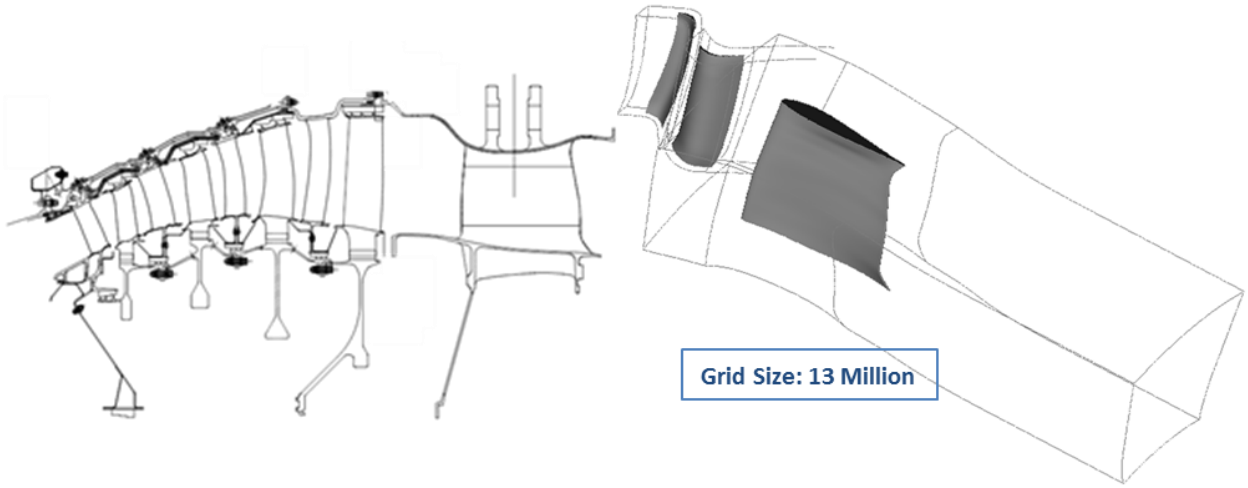

Figure 1. ANTLE Turbine (left) and CFD domain (right)

CFD simulation is performed for the second Blade Passing Frequency (BPF) emerging from the last stage, which is one of the dominant tone for this LPT. This tone is generated by the wake from the fourth vane interacting with the downstream rotor, generating noise being transmitted through the OGV. Since the gaps are sufficiently high, noise is predicted using LRANS calculations that can be described in the following steps:

- Steady aerodynamics are computed for the last stage and the OGV at Approach and Cutback noise representative conditions. Figure 1(right) shows the computational domain.
- Wake is extracted from the fourth vane aerodynamics and is imposed as a perturbation for the LRANS computation over the last rotor.

- Resulting acoustic and vorticity waves from the vane and rotor interaction are imposed at the OGV inlet in another LRANS calculation from which the acoustic energy is derived at the exit.

The Baldwin-Lomax(1978) turbulence model has been selected for this simulation. Fourth vane grid is optimized for predicting wake depth, that is 107 radial planes and structured boundary layer grid for achieving y+<1. Last rotor and OGV increases the radial planes to 130 for capturing the acoustic field, same criteria for the boundary layer grid and the inviscid region has a grid density of 40 points for the smallest wavelength of interest (Escribano et al., 2003). Overall grid size is 13 million nodes.

Figure 2(left) shows the predicted vs measured noise levels for the two working conditions. Approach prediction exceeds in around 2 dB the measured uncertainty whereas the Cutback estimate is within that interval. The Tyler&Sofrin (1962) interaction mode passing through the 14-off OGVs is 32; when being transmitted, a set of spinning modes raises according to the Tyler&Sofrin (1962) rule $m=32-k14$, where k is any integer. The set of cut-on spinning modes for both conditions is 46, 32, 18, 4, -10, 24 and -38. Each mode will carry different energy level depending on how the incoming mode 32 interacts with the OGV. The measured vs predicted results of that interaction are shown in Figure 2(center) for Approach and Cutback (right). It can be seen the same conclusion as in the overall energy, with the energy repartition well captured except for the spinning modes -10 and 46.

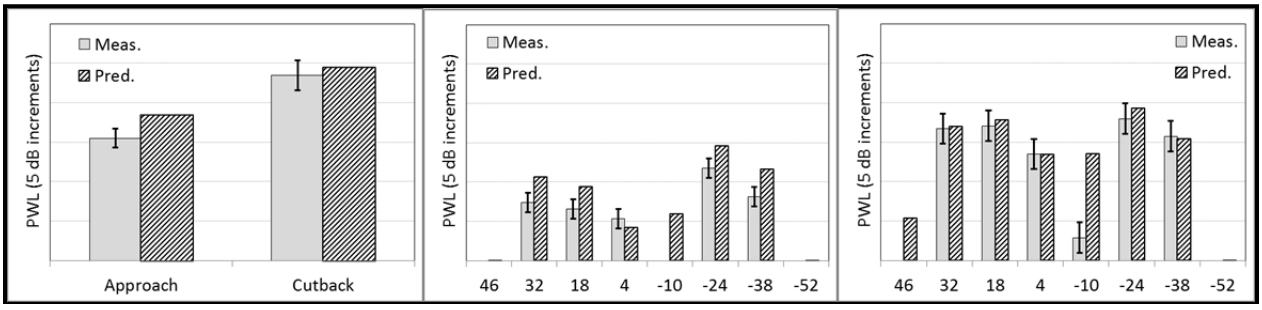

Figure 2. Predicted vs measured 2BPF tone from last stage: Overall energy (left) Modal decomposition at Approach (center) and at Cutback (right)

LINER PREDICITON CAPABILITY

CFD liner estimation capability is investigated in two cases: the first is a straight lined duct in presence of uniform axial flow, so that the results can be compared with that obtained using the semi-analytical solution based on the Bessel functions (Law, 2008). The second is a fan test in which noise measurements are taken with and without acoustic treatment on the pressure side of the OGV.

Lined Straight Duct with Uniform Flow

Test case considered has the following characteristics: Tip Radius = 0.458 m; Hub to Tip Ratio = 0.634; Treated Length to Tip Ratio = 0.791; Mach Number = 0.26; Frequency = 4836 Hz; Acoustic Impedance $Z / \rho c = 1.4268 - 0.3005i$; Spinning mode -6 and radial order 1.

Figure 3(right) shows the instantaneous pressure contours for the hard-walled (top) hub treated (middle) and hub and tip lined (bottom) configurations. Figure 3(left) shows the attenuation results for these two configurations referred to the hard-walled. Semi-analytical results are obtained from TURNOLINER, it is in-house code for liner optimization and

prediction of ducts with uniform flows. Mathematical formulation is based on an extension of Bessel formulation (Law, 2008). TURNOLINER capability for predicting liner benefits in hot engine ducts has been demonstrated by the comparison with existing engine measurements (Serrano, 2012).

CFD results from Mu^2s^2TL appearing in Figure 3(left) are presented in two ways: the first is the ratio between inlet and outlet amplitude for the same circumferential and radial mode (no scattering assumption). The second is based on the incoming level and overall up & downstream propagating energy. The scattering option includes acoustic reflections as the acoustic wave reaches the liner and the appearance of higher order radial modes carrying energy. This scattering is not modeled in TURNOLINER, and it assumes there is no reflection and/or energy into other radial modes. Consistency of TURNOLINER and Mu^2s^2TL can be observed since the semi-analytical values are in between the CFD results. Although not presented here, similar results have been achieved when assessing other flow conditions, spinning modes and radial orders in the duct.

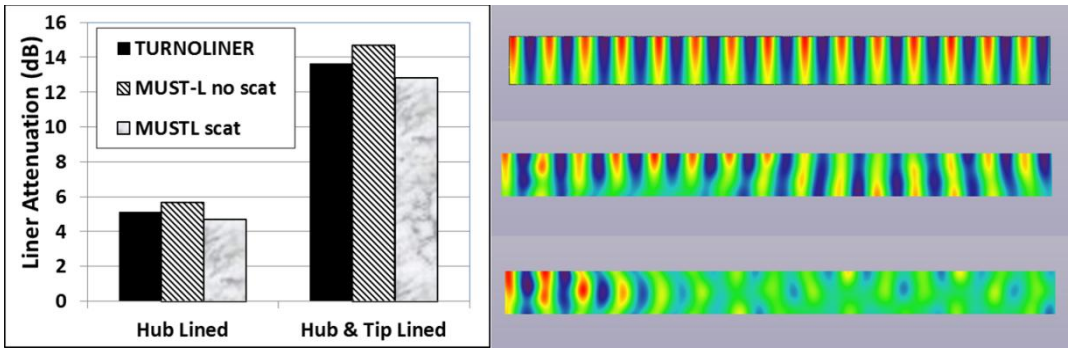

Figure 3. Predicted attenuations for the Lined Duct with Uniform Mean Flow (left). Instantaneous Pressure Contours for Hard-walled duct (right top) , hub lined (right middle) and hub & tip lined (right bottom).

Lined Fan OGV Test Case

Acoustic attenuation of the liner located on the pressure side of a fan OGV is predicted by the CFD and compared with available measurements. The experiment is conducted at the AneCom Facility in Germany during 2012 as part of the OPENAIR European Program. The AneCom AeroTest Universal Facility for Acoustics (UFFA) fan rig test facility includes intake, fan, OGV and bypass duct. The noise instrumentation consists of 180 rotating microphone array downstream the bypass duct. Noise measurements are conducted by AneCom and DLR including radial and circumferential mode detection (Tapken et al, 2011). Although this particular test cannot be found in the present literature, further details on a similar experiment can be found in Giacché et al (2013).

Noise analysis is performed in three operation points: Approach, Cutback and Sideline. CFD model used is LRANS and has the following steps:

- The aerodynamic flow is computed from the steady boundary conditions at the inlet OGV. Exit conditions are fed in the Bypass duct aerodynamic calculation.
- The fan wake is imposed at OGV inlet. Two set of LRANS cases are then generated depending on OGV that can be hard-walled or lined. The fan wake boundary condition has been previously predicted via CFD.

- Finally, an additional set of LRANS cases are computed for modelling the propagation of OGV exit noise through bypass duct, which is acoustically treated, until the measurement section where CFD results are compared with experiments.

Figure 4 (left) shows the computational domains. Blue areas corresponds to acoustic treatment whether in the OGV pressure side or Bypass duct. The build is split in two different parts, the OGV and the Bypass duct. The OGV mesh has the same grid criteria as in the ANTLE case: 130 nodes spanwise, boundary layer to achieve y+<1, and blade-to-blade grid size is selected to have 40 points per wavelength for the first BPF as done by Escribano et al, (2003). The resulting grid has 14.5 million nodes. The Bypass duct is simulated using an inviscid model. The acoustic treatment in the duct has impedance values including the grazing flow. The number of spanwise points is 125, uniformly distributed and able to propagate up to a third radial mode shape. The number of circumferential and axial points is chosen to propagate the first BPF spinning and radial modes, resulting in an overall grid size of 1.5 million.

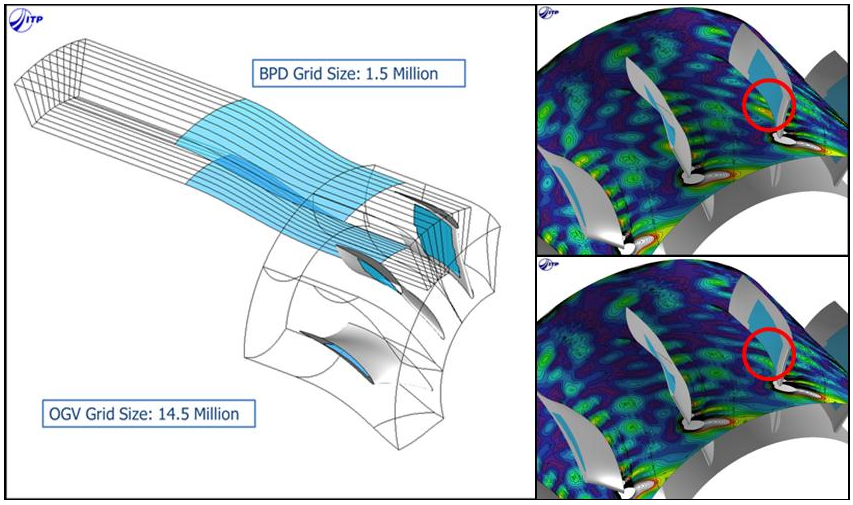

Figure 4. OGV and Bypass duct computational domain (left). Unsteady pressure amplitude contours for hard-walled (right top) and Lined (right bottom) OGV at Sideline. Blue areas refers to acoustic treatment.

Figure 4(right) shows two plot contours for the unsteady pressure amplitudes in the hard walled (right top) and lined (right bottom) cases, at Sideline conditions. The blue caps located at the pressure side correspond to the acoustically treated area. When observing the hard-walled computation (right top), there is an orange region in the pressure side, within the red circle, denoting high levels of unsteady pressure. However, the lined computation (right bottom) which has the same colour legend and scaling, the 'red circle' region has changed from orange to green, indicating the noise reduction due to the presence of the liner.

Figure 5(top) shows the predicted vs measured modal content for the hard-walled OGV, since it is an essential step for an accurate lined OGV prediction. Acoustic power (PWL) is presented for different cut-on modes at the exit according to the Tyler & Sofrin(1962) rule *B-kV*. Discrepancies between measured and predicted levels are within 5 dB, although there are some spinning modes miss-predicted up to 10 dB. Besides the CFD tool capability, another arguments can be given i.e., wake profile imposed at the inlet, steady flow accuracy, liner impedances

imposed at bypass duct or the acoustic coupling between the OGV and Bypass duct domains and boundary conditions.

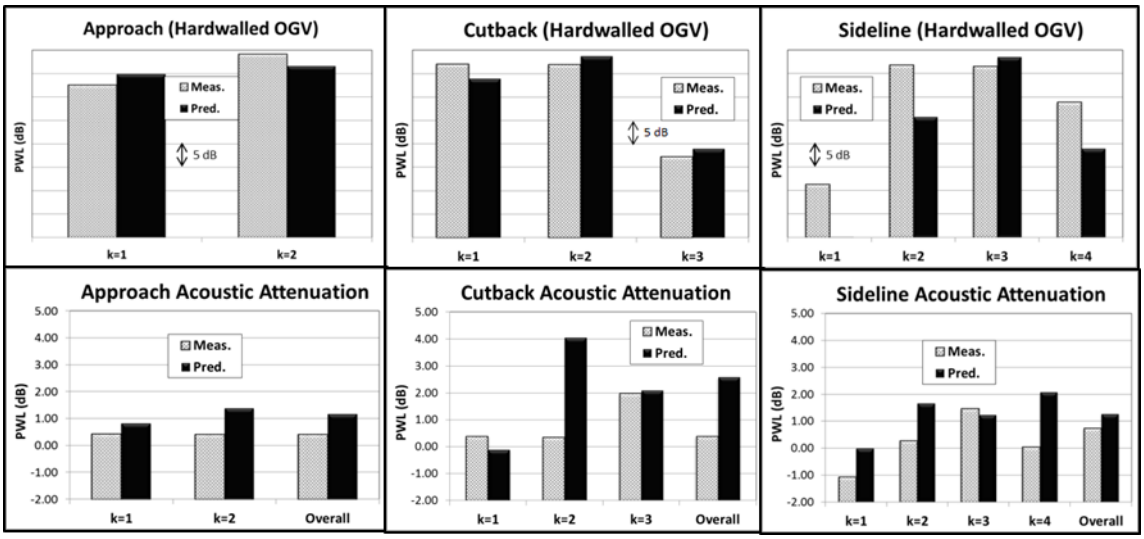

Figure 5. Predicted vs Measured modal content for the Hard-walled OGV(top) and Lined deltas (bottom) for the first BPF.

Figure 5(bottom) shows the results for the lined OGV assessment, expressed in deltas referred to the hard-walled calculations shown in Figure 5(top). Agreement between predictions and measurements are within 1 dB except for some particular spinning modes with miss-predictions up to 4 dB. Again, discrepancies can be due to the CFD but also other arguments can be given, i.e., hard-walled computations as discussed previously or the OGV liner impedances.

ESTIMATON FOR A LINED TURBINE OGV

The procedure consists in evaluating the lined OGV benefits for a state of the art 3-stage LP Turbine. Calculations are performed for one unique working condition that is in between Landing and Take-Off, hence the results are thought to be representative of the three noise critical conditions of Approach, Cutback and Sideline.

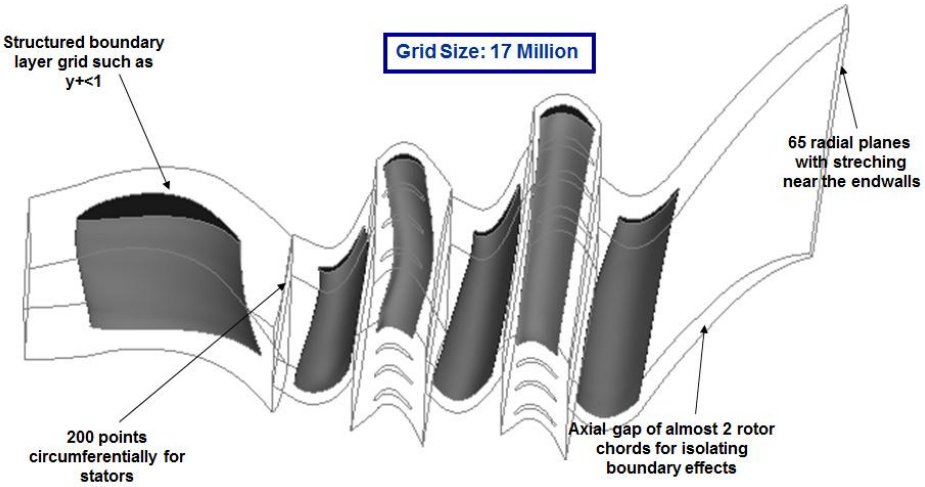

Figure 6. URANS Computational Domain for the 3-stage turbine

Figure 6 shows the turbine in absence of the OGV. Vane 1 chord is much larger than the other rows, and the gap to chord ratio is below the 40% critical ratio in which URANS and LRANS discrepancies starts to appear (Fernández et al., 2011). Consequently, a hybrid URANS and LRANS method is proposed consisting in the following steps:

- URANS computation of the 3-stage turbine until the OGV exit. Vane count in stages 2 and 3 is the same and four times the vane count in stage 1. Hence, the three stages has the same pitch when constructing a 1x4x4 CFD domain for the static part. On the rotatory side, blades in stages 1, 2 3 have the same count, and the 3-stage URANS can be done with an unique phase-lagged boundary condition (Burgos et al, 2011) between rotatory and static parts.
- Sources emerging from the URANS computation are transmitted thru the hard-walled OGV using independent LRANS calculations. Tone sources at first and second BPF at OGV exit are estimated.
- Optimum liner characteristics are obtained as if it were a liner over the hot nozzle and the usual cell depth vs porosity maps are obtained with TURNOLINER for the hard-walled sources derived from the CFD.
- Lined OGV computations: The same OGV hard-walled computations are done with the OGV acoustically treated.
- Tone noise delta estimations: CFD results are then applied for evaluating the entire effect of lined OGV for the turbine tones.

The next sub-sections describe in more detail each of these steps.

Turbine URANS Computation

Figure 6 shows the computational domain and grid characteristics used for the URANS simulation of the 3-stage turbine. As mentioned, the number of vanes and blades is such that same phase-lagged boundary conditions between stationary and rotatory parts are imposed for the three stages. Turbulence effects are accounted for using the Wilcox (1998) k-ω model. It has been changed from the Baldwin Lomax(1978) used in the ANTLE turbine for being the k-ω more appropriate to the particularities of this turbine. Vane and blade boundary layers have a structured grid that $y^+<1$. The number of points chosen in radial direction is 65, not ideal for aerodynamics or aeroacoustics but selected due to overall grid size limitations. The number of points in the circumferential direction has been chosen to pursue up to the fourth wake harmonic for the first vane and the second rotor BPF (Escribano et al, 2003). Third and so BPFs are not considered in the analysis for being out of the audible range. The overall grid size is 17 million nodes and the convergence criteria as previously investigated for similar cases (Burgos et al, 2011 and Fernández et al, 2012).

Figure 7, Figure 8 and Figure 9 shows at the three sliding planes located at each vane row exit, the time averaged contours of axial velocity, static pressure and entropy, respectively. When observing the axial velocity, contours at the first sliding plane are dominated by the first vane wake, and it is also prominent at the second plane together with the second vane wakes. That suggests Vane 1 will generate noise when interacting with Blade 1 but also with the rear stages. This Vane 1 wake is still appreciable at Vane 3 exit. Pressure contours behave quite differently and the potential field emerging from Vane 1, clearly visible in the first sliding plane, decay exponentially and cannot be noticeable in the downstream sliding planes. Finally, entropy contours emerging from Vane 1 are observed with similar intensity in Vane 2 and 3 exit, as would be expected since the entropy is not subject to any mixing and/or decay effects.

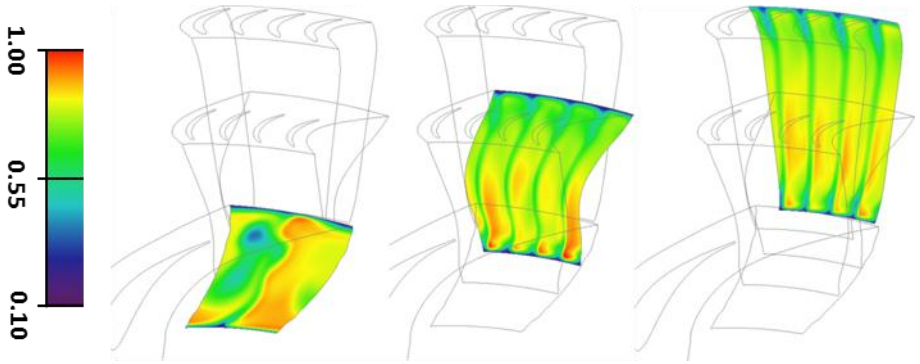

Figure 7. Time averaged axial velocity contours at the three sliding planes. Scale referred to the maximum level.

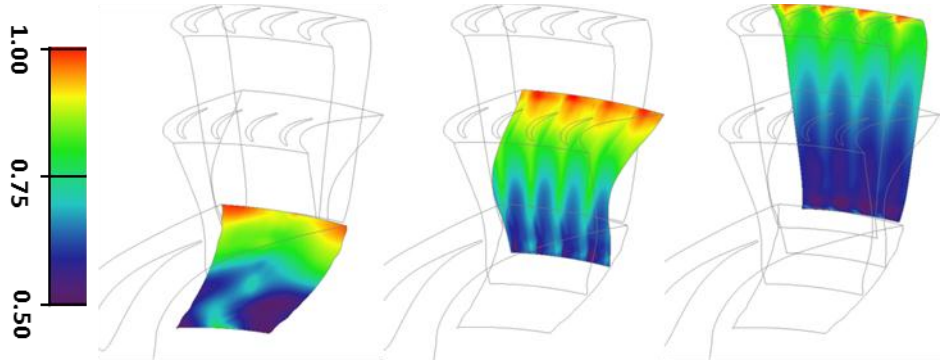

Figure 8. Time averaged pressure contours at the three sliding planes. Scale referred to the maximum level.

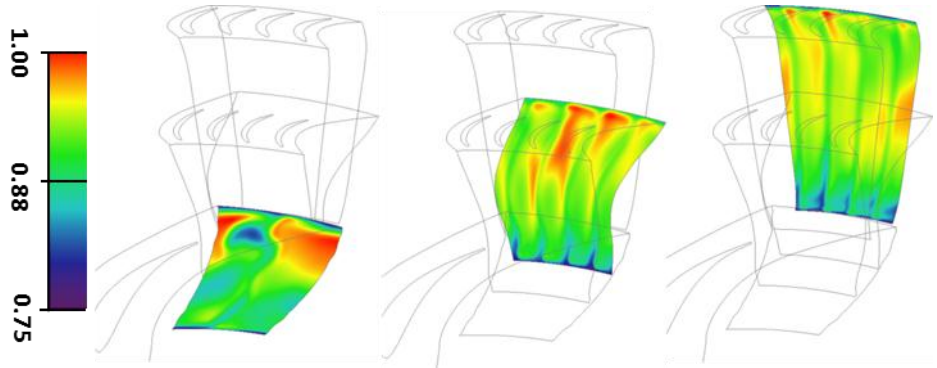

Figure 9. Time averaged entropy contours at the three sliding planes. Scale referred to the maximum level.

Hard-walled OGV LRANS Computations

The perturbations from the URANS computation are imposed at the OGV inlet and independent LRANS calculations are performed. Grid characteristics are consistent with those described for the URANS computation. The overall grid size for the OGV is 2.5 million nodes.

Figure 10(right) shows the instantaneous unsteady field for two of these computations. The top-right plot corresponds to one of the two incoming vorticity waves and the flow variable is the velocity. The bottom-right one is an incoming acoustic wave where the variable is unsteady pressure.

In order to understand the OGV role in the turbine noise generation, Figure 10(left) shows the noise sources for the first BPF with and without the OGV. According to the Tyler & Sofrin rule (1962), the interaction between the blade and vane rows within the LPT will result in a set of spinning modes of *B-kV* contributing to the first BPF, being *k* any integer. For the investigated working condition, there are only cut-on modes for *k* values of 2 (2 radial modes at OGV inlet and exit), 3 (4 radial modes at OGV inlet and exit) and 4 (cut-off at OGV inlet and 2 radial modes at OGV exit). Calculations in the absence of the OGV will result in acoustic energy being distributed in *k*=2 and *k*=3, being similar in importance. When considering the OGV, the vortical and entropy sources emerging from the LPT will need to be accounted besides the cut-on acoustic energy. Figure 10(left) illustrates how different is the OGV role in turbine noise compared with fans, consequently the convenience of using a liner might be different as well.

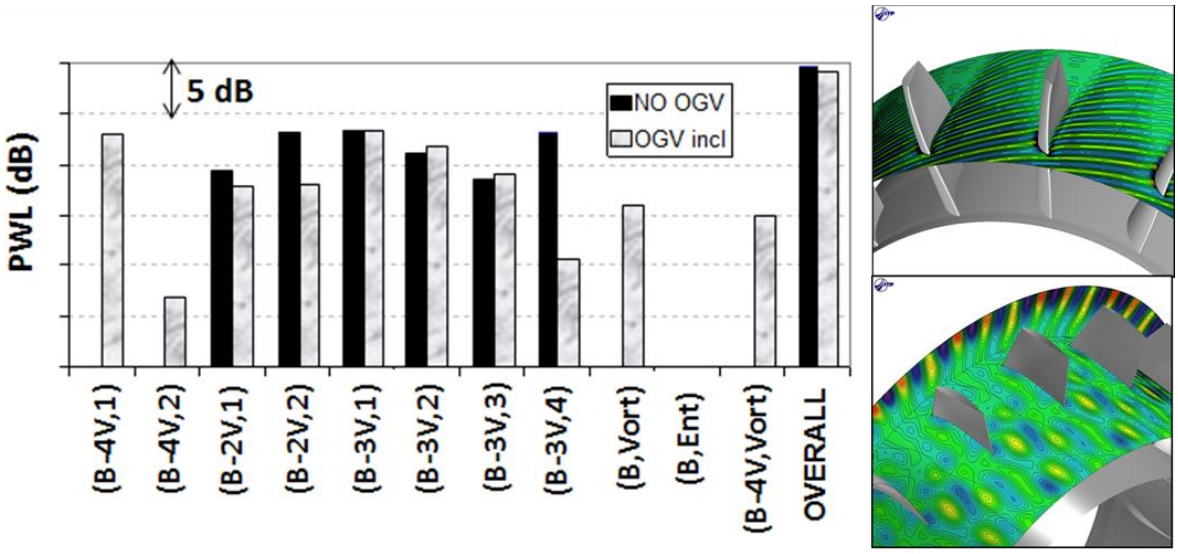

Figure 10. 1BPF Noise Source Breakdown with and without OGV for the Hard-walled Case (left). Instantaneous unsteady field for velocity and incoming vorticity(right top) and pressure and incoming acoustic(right bottom).

Liner Optimization

Next step is defining the liner characteristics to be simulated. TURNOLINER is run for the hard-walled OGV exit tone sources, being attenuated through different lined nozzle duct candidates, and then broadened up to the engine exit using a 'haystacking' tone model as reported by Serrano et al.(2012).

Perceived Noise Level with Tone correction (PNLT) has been chosen as the most appropriate metric to evaluate engine noise in absence of flight effects. Results obtained are shown in Figure 11(left) and selected liner characteristics in terms of cell depth has been checked with the mid-span OGV section (right). Optimum length is compatible with the airfoil thickness but the use of treatment in both pressure and suction sides is not feasible. Hence, the investigation of which side is more appropriate from a noise point is addressed. Besides, it is doubtful that all the acoustic area shown in Figure 11(right) will be affordable due to other constraints, something that will not be addressed in this work. Alternatively, an area reduction of 70% referred to the overall treated (suction or pressure) area has been assumed.

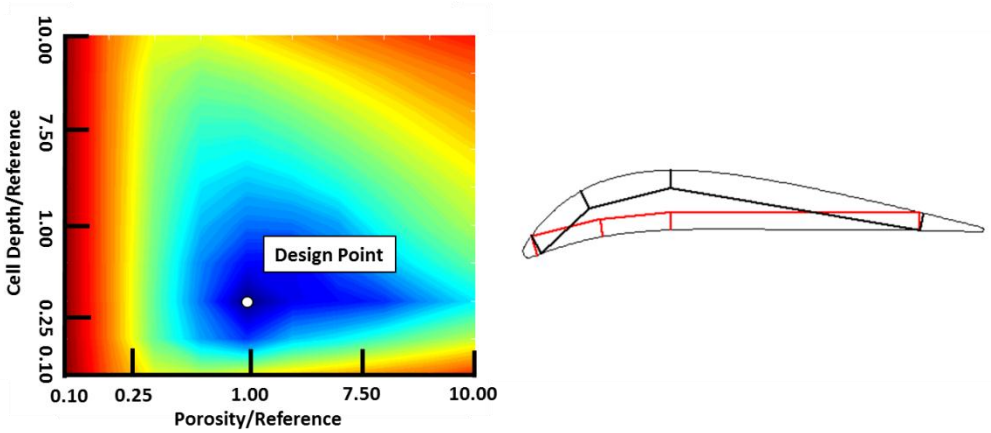

Figure 11. Optimization of liner charact. and fitting sketch on the mid span section.

Lined OGV Computations and Tone Delta Estimations

The same calculations performed for the hard-walled OGV are done in presence of the acoustic liner in the suction or pressure sides. The resulting deltas are shown in Figure 12(left). It also shows the calculated deltas for the same liner characteristics but over the downstream plug surface as previously done in other engines (Chien, 2009, Serrano, 2012). In the suction side, the delta observed for 1BPF and 2BPF varies greatly, this is because the latter is dominated by counter-rotating spinning modes. However, 1BPF is more influenced by the rotor wake and a mix of co & counter rotating modes so that the pressure side treatment looks more effective. In this exercise, the suction side treatment seems to be more convenient although the advantage over the pressure side is not high.

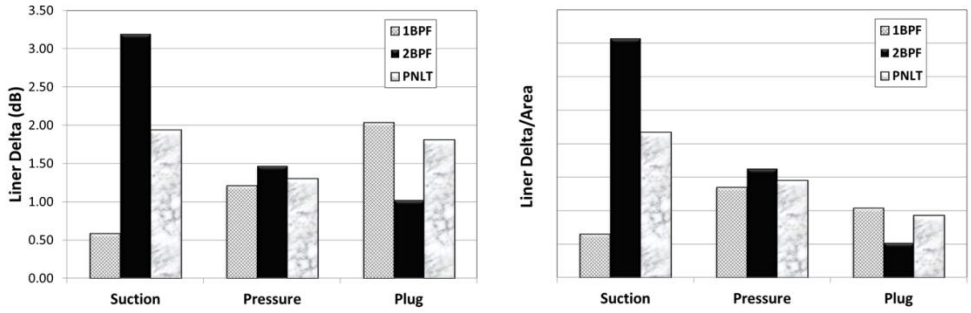

Figure 12. Liner delta predictions (left) and deltas per unit treated area (right).

Figure 12 (right) shows the same deltas but expressed by unit treated area. This demonstrates that, although the absolute PNLT deltas obtained in the suction side and plug are similar, the wetted area used in the plug treatment is more than twice, consequently, the lined OGV surface results are more effective than in the plug nozzle.

CONCLUSIONS

Acoustic treatment over OGV airfoil surfaces has been addressed by several authors for fan noise (Reba et al. 2008, Elliot et al. 2009, Jones et al. 2009) but the application for turbines has not been found in the literature. In absence of a dedicated experiment, estimations via CFD have demonstrated that this technology can conduce to similar benefits than other already demonstrated practices as treated plugs in the engine.

The CFD capability for assessing this technology has been assessed in two parts. First, turbine tones prediction; CFD has been compared against noise measurements from the ANTLE turbine rig, including the OGV, and estimations are mostly within measurement uncertainties. Second, liner benefits prediction; two test cases have been discussed, a straight duct with uniform flow, where CFD results have been successfully compared against a semi-analytical formulation, and a fan noise test case with a lined OGV where CFD is mostly within 1 dB discrepant with measured liner benefits investigated. It is important to note however that the CFD tends to over predict by one or few dB the lined OGV benefits and this could also happen in the turbine case.

The lined turbine OGV technology has been assessed for a state of the art 3-stage vehicle. Turbine characteristics are such that the noise sources have been estimated by unique multi-stage URANS calculation. Transmission thru the OGV has been modelled using independent LRANS calculations for each noise sources emerged from the turbine. The solution shows a strong interaction between stages resulting in a broad range of noise sources passing through the OGV.

The optimum liner characteristics for the turbine have been derived by constructing the usual cell height vs porosity maps for the hard-walled sources. Optimum liner depth is compatible with the airfoil thickness but will only allow treatment in one airfoil side. Liner CFD predictions when installing treatment in the pressure or suction side have been derived and compared with that benefits on a lined plug. There is a great dependence on the modal content so that wakes and co-rotating modes are well attenuated in the lined pressure side whereas counter-rotating modes are better attenuated with the treated suction side. The optimum solution will be case dependent. Furthermore, liner OGV results are twice more effective than a treated plug since it requires 50% less area for similar attenuations.

Once the relevance of this technology has been demonstrated, several future work directions have been identified. First, investigating further the capability of the CFD for lined OGV predictions, distinguishing which are related to the CFD and which to other sources. Second, mechanical issues will be also highly relevant, as in fans, plus additional issues related to the hot temperature environment and smaller sizes. Other issues related to the actual design of the liner in order to achieve the desired impedance and aerodynamics effects will also need to be addressed.

ACKNOWLEDGEMENTS

The ANTLE turbine analysis, and 3-stage URANS calculations and analysis have been funded by ITP. The liner calculations have been funded by ITP and the 7th Framework Program OPENAIR under grant agreement n° 234313. The fan experiment has been provided by OPENAIR. The state of the art turbine geometry and boundary conditions has been provided by Rolls-Royce.

REFERENCES

Baldwin, B.S., Lomax, H., *Thin Layer Approximation and Algebraic Model for Separated Flows*, AIAA Paper, 78-257, 1978.

Broszat, D., Tapken, U., Enghardt, L., Legani, D., Marn, A., *Validation of an Integrated Acoustic Absorber in a Turbine Exit Guide Vane*, AIAA Paper, 2011-2915.

Burgos, M.A., Contreras, J. and Corral, R., *Efficient Edge-Based Rotor/Stator Interaction Method*, AIAA Journal, Vol. 49, No. 1, pp 19-31, January 2011.

Chien E.W., Ruiz M., Yu J., Morin B.L., Cicon D., Schweiger P.S., Nark D.M., *Comparison of Predicted and Measured Attenuation of Turbine Noise from Static Engine Test*, AIAA paper, AIAA-2009-3144.

Corral, R., Escribano, A., Gisbert, F., Serrano, A., and Vasco, C., *Validation of a Linear Multigrid Accelerated Unstructured Navier-Stokes Solver for the Computation of Turbine Blades on Hybrid Grids*. AIAA Paper 2003-3326.

Elliot, D.M., Woodward, R.P., Podboy, G.G., *Acoustic Performance of Novel Fan Noise Reduction Technologies for a High Bypass Model Turbofan at Simulated Flight Conditions*, AIAA Paper, 2009-3140.

Escribano, A.G., Serrano, A. and de la Calzada, P., *Investigation on Numerical and Geometry Modelling Effects on the CFD Simulation of Interaction Noise in LP Turbines*. 5th European Conference on Turbomachinery Fluid Dynamics and Thermodynamics. Prague, Czech Republic. March 2003.

Escribano, A.G., Serrano, A., Vasco C., *Cascade-Gust Interaction Problem Analysis based on Linear CFD Calculations*. 4th AARC Workshop on CAA Benchmark Problems, Cleveland, OH, October 2003.

Fernández Apararicio, J.R., Serrano, A., Vázquez, R., *On the Linearity of Turbomachinery Interaction Noise. Part I: 2D Analysis*, AIAA Paper, 2011-2951.

Fernández Apararicio, J.R., Serrano, A., Vázquez, R., *On the Linearity of Turbomachinery Interaction Noise. Part II: 3D Analysis*, AIAA Paper, 2012-2309.

Jones, M.G., Parrot, T.L., Sutliff, D.L., Hughes, C.E., *Assessment of Soft Vane and Metal Foam Engine Noise Reduction Concepts*, AIAA Paper, 2009-3142.

Giacché, D., Hynes, T., Baralon, S., Coupland, J., Humphreys N., and Schwaller, P., *Acoustic Optimization of Ultra-Low Count Bypass Outlet Guide Vanes,* AIAA Paper 2013-2295.

Law, T.R., *Multi-Segmented Liner Optimisation for Mixed Exhaust Aeroengines*, PhD Thesis, University of Cambridge, UK, 2008.

Nesbitt, E., *Towards a Quieter Low Pressure Turbine: Design Characteristics and Prediction Needs*, International Journal of Aeroacoustics, Vol 10., No 1, pp 1-15, August 2010.

Reba, R.A., Morin, B.L., *The Gust Response of an Acoustically Treated Flat-Plate Cascade*, AIAA Paper 2008-2898.

Serrano, A, Fernandez J.R., Vázquez, R, Moore A.D., "Data Reduction Techniques for a Low Pressure Turbine Noise Test", AIAA paper, AIAA-2007-3713.

Serrano A., *Linearized CFD Techniques applied for Low Tonal Noise Designs in Turbines*, Proceedings from the AARC Workshop in Turbine Noise, Vancouver, BC, 2008.

Serrano, A, Vázquez, R., "Feasibility of Using Single Mode Rings for the Characterization of Turbine Tone Noise", AIAA paper, AIAA-2011-2911.

Serrano, A., Vázquez, R., Moore, A.D., *Investigation on Turbine Tone Broadening in Static Engines*, AIAA Paper 2012-2305.

Tapken, U., Bauers, R., Neuhaus, L., Humphreys, N., Wilson, A. G., Stöhr, C., and Beutke, M., *A New Modular Fan RigNoise Test and Radial Mode Detection Capability*, AIAA paper 2011-2897.

Tyler, J.M. , Sofrin, T.G., *Axial Flow Compressor Noise Studies*. SAE Transactions, Vol 70, pp 309-332, 1962.

Vázquez, R., Cadrecha, D., Torre, "High Stage Loading Low Pressure Turbines". A New Proposal for an Efficiency Chart, ASME paper, 2003, GT2003-38374.

Wilcox, D. C., *Turbulence Modeling for CFD*, DCW Industries, Philadelphia, 1998.